Experimental Correlation Between Microstructure, Residual Stresses and Mechanical Properties of Friction Stir Welded 2024-T6 Aluminum Alloys

Majid Farhang, Mohammadreza Farahani *
School of Mechanical Engineering, College of Engineering,
University of Tehran, Tehran, Iran
E-mail: m_farhang@alumni.ut.ac.ir, mrfarahani@ut.ac.ir
*Corresponding author

Mohammad Nazari
School of Mechanical Engineering, University of Tehran, Tehran, Iran
E-mail: Mohammad_nazari@ut.ac.ir

Omid Sam-Daliri
Department of Mechanical Engineering, National University of Ireland, Galway, H91 TK33, Ireland, E-mail: omid_sam@nuigalway.ie

Received: 1 November 2021, Revised: 16 April 2022, Accepted: 23 April 2022

Abstract: Friction stir welding was performed on AA2024- T6 aluminum plates using different rotation and traverse speeds with the objective of improving the mechanical strength and microstructure properties. The influence of the traverse and rotation speed on the microstructures, mechanical properties and residual stresses of the welded Aluminum plates were investigated. By increasing the rotation speed, stirred zone grain size became larger. Besides, the homogenous second phase distribution was obtained. Furthermore, by increasing both rotational and traverse speeds, hardness of the thermo-mechanically affected zone and the stirred zone increase to base metal hardness. These welded plates that were fractured at advancing side have a maximum tensile strength equal to 71% of base plate strength which was obtained at 31.5 mm/min traverse speeds and 1120 rpm rotational speed. The longitudinal residual stress was diminished with decreasing of rotational speed by 1120 rpm at a constant traverse speed. In this conditions and by increasing the traverse speed by 31.5 mm/min, the maximum tensile strength was obtained as many as 48%. It was attributed to more plastic deformation and minimum grain size in the weld zone due to higher traverse speed.

Keywords: Al 2024-T6, Friction Stir Welding, Mechanical Properties, Residual Stress

How to cite this paper: Majid Farhang, Mohammadreza Farahani, Mohammad Nazari, and Omid Sam-Daliri, "Experimental Correlation Between Microstructure, Residual Stresses and Mechanical Properties of Friction Stir Welded 2024-T6 Aluminum Alloys", Int J of Advanced Design and Manufacturing Technology, Vol. 15/No. 3, 2022, pp. 1-9. DOI: 10.30486/admt.2022.1943845.1322.

Biographical notes: Majid Farhang received his MSc form University of Tehran in 2015. His research topics are welding, residual stress & manufacturing. **Mohammadreza Farahani** received his PhD in Mechanical Engineering from Amir Kabir University of Technology in 2010. He is directing the TWN Lab. His research interests include Non-destructive tests in welding and composites joints. **Mohammad Nazari** received his MSc from University of Tehran. He has shown great interest in metallurgical and mechanical joints. **Omid Sam-Daliri** received his PhD in Mechanical engineering from University of Tehran in 2014. He is a postdoctoral researcher un ASMME group at University of Galway, Ireland. His research interest are fracture mechanics, advanced composite materials, welding and manufacturing.

1 INTRODUCTION

Mechanical and microstructure properties of aluminium components have an important role when they employ in engineering structures. Fatigue strength, corrosion resistance and fracture type of the metallurgical joints are under the influence of tensile strength, hardness and Residual stress. Traditional welding processes make non-uniform thermal distribution in welding area which it has induced by residual stress. Therefore, it diminishes the component life. Great demands on new manufacturing process with low residual stress has created Friction stir welding (FSW) method. This technique is a solid-state welding method that involves heating the base metal to the plastic zone. The residual stresses in FSW welds are lower than those generated during fusion welding, but they are not negligible at all. FSW is widely being implemented by many industries such as aerospace, automotive, rail transportation and shipbuilding industries, particularly for the aluminium alloys [1-2]. It has represented that FSW process produces low distortion and residual stress and produced high performance joints in comparison with the conventional welding processes [3-6]. The studies represent that the FSW has been conducted at lower temperature with respect to the melting temperature of the base metal. So this welding process categorized as a kind of solid state joining process [7-8], in which the solidification microstructure containing brittle phases and porosities will be diminished. In FSW, a tool (with shoulder and pin) penetrates into the interface of two adjacent plates with a rotation speed and travels along this interface. The surrounding material of the tool is heated and softened by friction made by the tool. It causes a high plastic deformation or a nugget zone in the welding line to be comprised. Therefore, it can be employed for joining of similar and dissimilar materials [9-11]. By stirring action in FSW, two different regions at both side of weld zone were observed. The advancing side is the side where the tool rotation and traverse movement are acting in a same direction. The other side is retreating side. Each weld side consists of three regions named stirred zone (SZ) also known as dynamically recrystallized zone or nugget zone, the thermo-mechanically affected zone (TMAZ) and heat affected zone (HAZ) which have different microstructure [12-14]. Some studies on FSW has been performed to evaluate the microstructure changes, strength, hardness, and weld residual stress, separately under static and fatigue load [15-17]. Based on the literature, the joint properties were affected significantly by the high temperature rather than the plastic deformation [18-19]. Segregated band with hard particles can be found in microstructure of FSW joint of 2024-T351 [20]. Moreover, the properties of FSW of 2024-7075 aluminium alloys are evaluated [21]. The effects of residual stresses were also investigated. It was found that the remained stresses had a greater impact on life time of aluminium joints rather than its influences on the hardness and weld microstructure [4], [22-24]. Farhang et al. [25] have studied the effect of manufacturing parameters on the remained residual stresses in the FSW of aluminium joint. However, the correlation between microstructure and manufacturing parameters has not been presented. Bachman et al. [26] have inverstigated the effect of different welding speeds on the residual stresses in FSW of aluminium alloy. Based on the reviews of the literature presented in this paper, there have been lack of study in the interrelationship analysis of microstructure, residual stresses and mechanical properties in FSW process which it needs more investigation.

In this study, the properties of FSW joint of AA2024-T6, an aluminum alloy which are mostly used in the aerospace industry was investigated and its residual stress distribution, mechanical strength and the weld microstructure were evaluated. Samples were welded at different rotation and traverse speeds as manufacturing parameters. The microstructure of each sample was examined, while a tensile and hardness tests were also conducted to assess the mechanical properties of the joints. In addition, the remained stresses were measured using hole-drilling strain gage method. In the last stage, the effect of manufacturing parameters has been investigated.

2 EXPERIMENTAL PROCEDURE

The experimental test was performed on eight rectangular plates from 2024-T6 aluminum alloy [27-29], with 150×50 mm dimensions and 4 mm thickness. The chemical composition and mechanical properties of the base metal were reported in "Table 1 and 2", respectively.

Table 1 Chemical Composition of Al 2024-T6 base metal

Element	Al	Mg	Mn	Cu	Si	Fe
Mass (%)	Remaining	1.57%	0.613%	5.32%	0.0973%	0.284%

Table 2 Mechanical Properties of Al 2026-T6 base metal

	Tensile Strength	Yield Strength	Hardness
Al 2024-T6	495 (MPa)	375 (MPa)	153(Hv)

The plates were FSWed by H13 steel tool with hardness of 56 HRC. The tool was made of shoulder and pin. Shoulder diameter was 16 mm and with height of 11mm. Elangovan et al. [30] showed that the square pin gives

more hardness and strength in welded area. Krishna et al. [31] evaluated the effect of using the different tool pin profile of friction stir welding on the mechanical properties of Al plates. They concluded that better mechanical properties of welded joint can be obtained by employing square tool, so we used this type of pin shape for the experiment. The pin of the tool had a square section with length of 4 mm and height of 3.85 mm. The overall height of the tool was 56.85. The tool tilted by 3 degree from the normal direction of the plate. The weld performed parallel to the rolling direction of the plates. Figure 1 shows the FSW process with employed tool in different views. The welding parameters of the prepared specimens are shown in "Table 3" (two samples were provided at each condition). The ranges of welding speeds were extracted according to the reported optimized welding parameters achieved in related studies to achieve the specimens without defect [32-33].

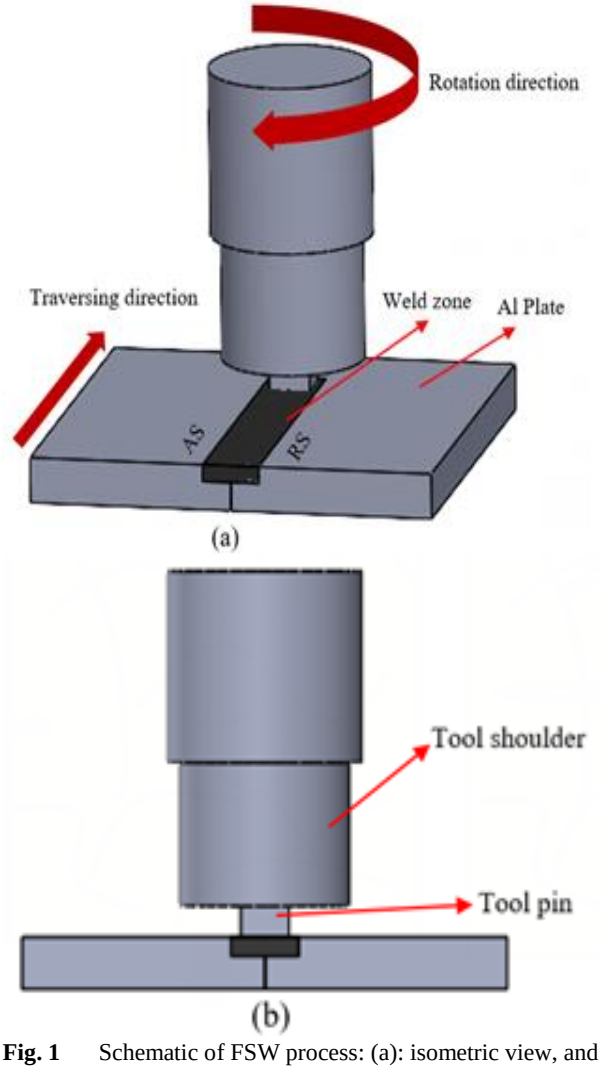

Fig. 1 Schematic of FSW process: (a): isometric view, and (b): front view.

Table 3 Welding parameters

Specimen	Rotation Speed	Traverse Speed
R1120-T25	1120(rpm)	25(mm/min)
R1120-T31.5	1120(rpm)	31.5(mm/min)
R1600-T25	1600(rpm)	25(mm/min)
R1600-T31.5	1600(rpm)	31.5(mm/min)

For microstructural studies, samples were extracted from welded plates. After polishing the surface of samples, they were etched by modified Keller etchant (3 ml HCl, 2 ml HF, 190 ml H_2O, 5 ml HNO_3,) and were examined by optical microscopy. The micro-hardness was measured along the cross section of the center line under the load and time of 0.5 N and 15 Sec, with an interval of 1 mm.

Tensile test was also conducted on a calibrated test machine (SANTAM) operated in displacement control with 50 KN load cell and 1 mm/min speed. The tensile test specimens were cut from the region indicated in "Fig 2" in direction perpendicular to the weld line. Three tensile samples were extracted and used to evaluate tensile properties of each specimen [34]. Figure 2 shows the dimensions and locations of each test sample.

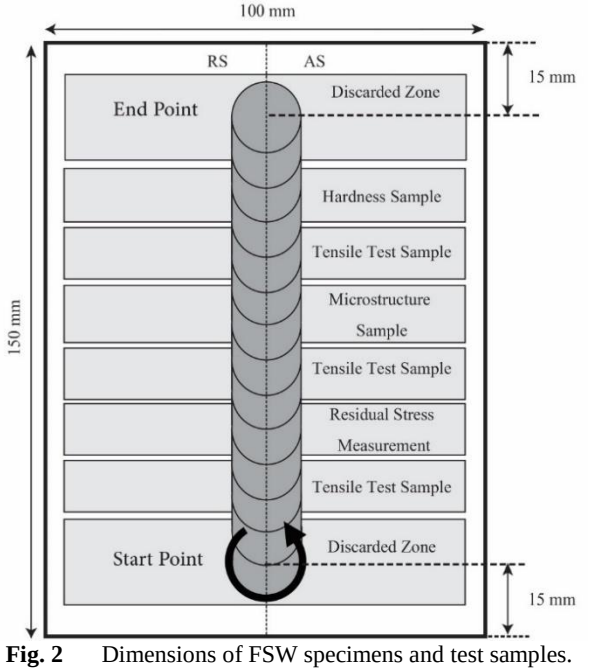

Fig. 2 Dimensions of FSW specimens and test samples.

Measurement of the residual stress has been performed using hole-drilling strain gage method [35-37]. Strain gauge based technology is used commonly in the manufacture of pressure sensors [38-41]. Measurements

were made in three points for each specimen. As it is shown in "Fig. 3(a)", one point on the weld centerline (SZ) and two other points on 8 mm distance away from the weld centerline on the boundary of SZ and base metal were selected. Rosette type strain gage was installed on the chosen points. The released strains during drilling are measured according to ASTM E837 standard [42]. Traverse and longitudinal remained stresses were calculated as Equation (1):

$$\sigma_{\min,\max} = \frac{\varepsilon_1 + \varepsilon_2}{4A} \mp \frac{1}{4B}\sqrt{(\varepsilon_3 - \varepsilon_1)^2 + (\varepsilon_3 + \varepsilon_1 - 2\varepsilon_2)^2} \quad (1)$$

Where, $\varepsilon_1, \varepsilon_2$ *and* ε_3 are the released strains from rosette strain gauges. Mechanical properties of the base metal and the hole diameter were counted by A and B coefficients. These coefficients are derived directly from the tables presented in ASTM E837 in accordance with Young's modulus and Poisson's ratio of the specimen and the diameter of the drilled hole. Figure 3(b) shows the hole-drilling strain gage measurement setup.

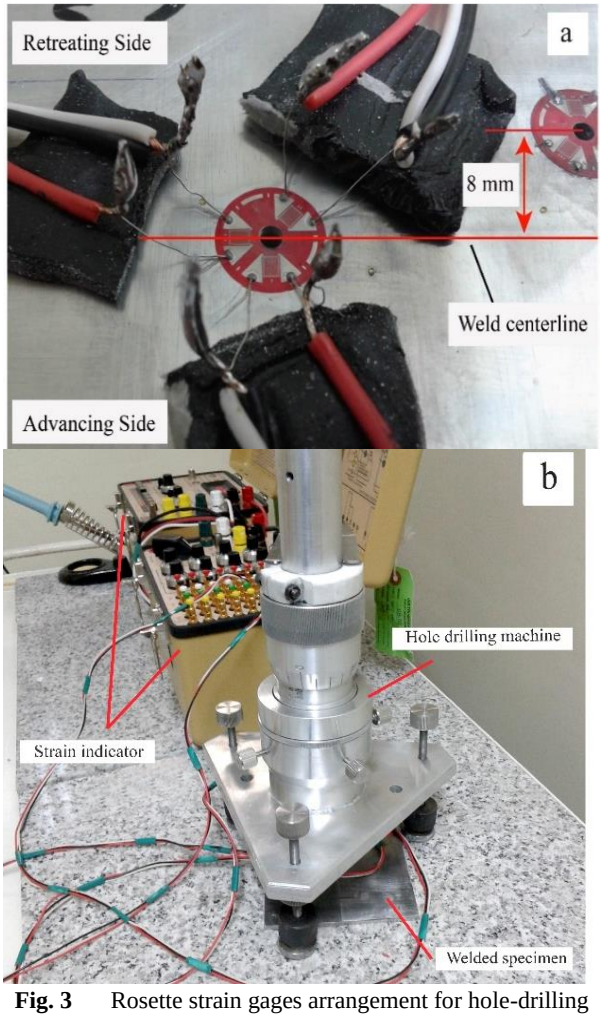

Fig. 3 Rosette strain gages arrangement for hole-drilling method.

3 RESULTS AND DISCUSSION

Rotation and traverse speeds of FSW process affect the properties of the weld zone. The following sections are concentrated on the microstructure, RS, tensile strength and hardness interrelationship of AA2024-T6 aluminum alloy FSW.

3.1. Microstructural Analysis

Based on the visual inspection before and after the tensile test, it was observed that all joints are free from defects like voids and tunnels. FSW joints are microstructurally divided into four regions: SZ in center line of weld, TMAZ, HAZ and Base metal. By changing the rotation and traverse speeds, due to different plastic deformation and welding temperature, the size of these zones changed subsequently.

Microstructures of different regions for specimen with 31.5 mm/min traverse speed and 1600 rpm rotation speed are shown in "Fig 4". Figure 4(a) shows the microstructures of weld zone and base metal. This figure indicates fine and elongated grains of base metal as a result of rolling process with second phase particle arbitrary distribution as represented in previous studies [42-44]. Figure 4(b) represents the microstructure of retreating side TMAZ. Besides, it is an evidence of plastic deformation which can be seen in TMAZ, it's likely not enough for occurring recrystallization. As a result of higher generated heat and plastic formation, fine, homogenous, recrystallized and equiaxed grains are demonstrated in SZ microstructure ("Fig. 4(c)"). The localized precipitation on grain boundaries provide suitable location for recrystallization phenomenon [45-46]. So this condition with low heat input lead to grain refinement. Figure 4(d) illustrates the microstructure of the bottom region of the joint section. It contains onion rings patterns resulted from non-homogenous distribution of refined grains and enhancement of dislocation density.

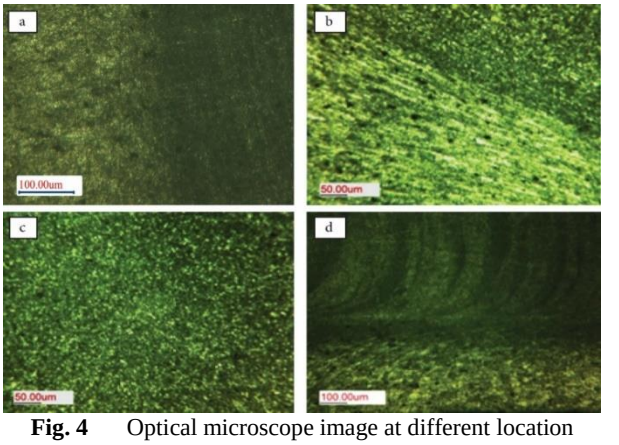

Fig. 4 Optical microscope image at different location corresponding to 31.5 mm/min traverse speed and 1600 rpm rotation speed: (a): weld zone and base metal, (b): retreating side of TMAZ, (c): SZ, and (d): bottom region of weld joint.

Figure 5 represents the SZ microstructures of different specimens. Increase in rotation speed and decrease in traverse speed made larger grains. Consequently, it caused smaller and more integrated distributions of second phase particles. The relation between FSW speeds and grain size is represented in "Table 4". "Table 4" shows the maximum grain size achieved at lowest traverse speed of 25 mm/min and the highest rotation speed of 1600 rpm.

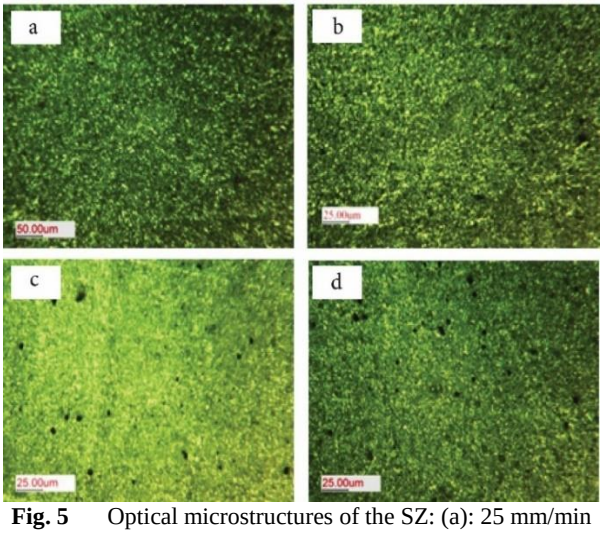

Fig. 5 Optical microstructures of the SZ: (a): 25 mm/min and 1120 rpm, (b): 31.5 mm/min and 1120 rpm, (c): 25 mm/min and 1600 rpm, and (d): 31.5 mm/min and 1600 rpm.

Table 4 Average grain sizes in the nugget zone at different rotation and traverse speeds

Specimen	Grain Size (μm)	Traverse Speed (mm/min)	Rotation Speed (rpm)
R1120-T25	1.73	25	1120
R1120-T31.5	1.35	31.5	1120
R1600-T25	2.67	25	1600
R1600-T31.5	2.41	31.5	1600

3.2. Hardness Measurement

Figure 6 illustrates the profiles achieved from micro-hardness test of the welded joints.

The hardness increases by increment of traverse speed. In constant rotation speeds (1120 or 1600 rpm), by changing the traverse speed from 25 to 31.5, the average of hardness increased about 6% similarly. In constant traverse speeds (25 or 31.5 mm/min), by increasing the rotation speed from 1120 rpm to 1600 rpm, the hardness values decreased about 19%. On the other hand, as stated in previous section, by increasing rotational speed and decreasing traverse speeds, the grain size increases subsequently. Regularly, the strength and hardness of high angle grain materials, decreases with increase of grain size. However, in this case, it can be inferred that the hardness is independent from the grain size [44], [47]. Here, there are second phase particle, precipitates size, distribution and plastic deformation during welding that characterize the weld hardness. In general, for age hardening aluminum alloys, amount, size and distribution of precipitates have a key role on the weld properties [48]. Increasing the tool traverse speed leads to higher plastic deformation and more uniform second phase particle distribution. It leads to higher hardness which may attributed to minimum grain size because the increase in tool traverse speed made more plastic deformation and consequently reduces the grain size.

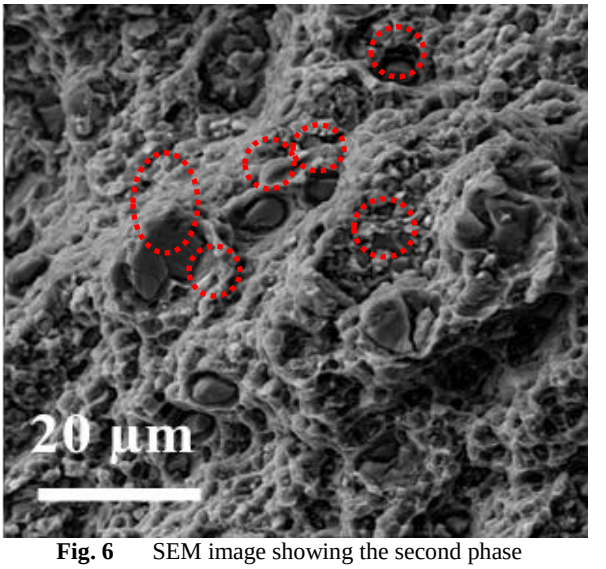

Fig. 6 SEM image showing the second phase precipitation.

3.3. Joints Tensile Strength

Tensile strength of welded specimens are shown in "Table 5". It can be seen, although the tensile strength of these specimens has not reached to the strength of base metal, it has improved by decreasing the welding speeds. It has observed that the tensile properties of friction stir welded joints without defect were proportional to hardness values and as stated before, the hardness depends on second phase particles distribution and induced from plastic deformation [44], [49]. Tensile strength reaches to its maximum value at 31.5 mm/min and 1120 rpm which has had the minimum grain size.

Table 5 Tensile strength of different welded specimens

Specimen	Tensile Strength (MPa)	Strain
R1120-T25	271	6.5
R1120-T31.5	325	9.6
R1600-T25	169	1.9
R1600-T31.5	199	2.4

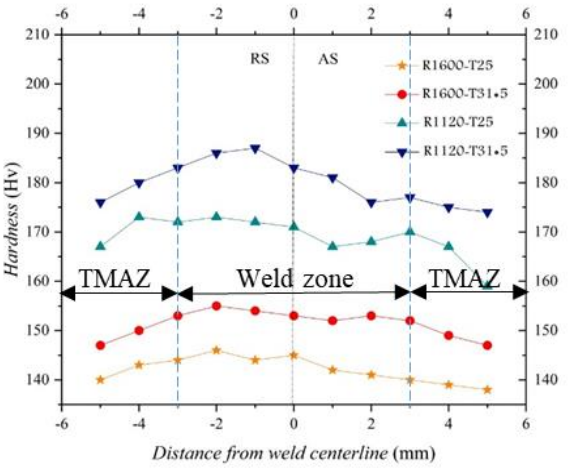

Fig. 7 Hardness profiles (transverse directions, mid thickness).

It can be seen that better distribution of second phase and higher plastic deformation has been made by increasing the tool rotational speed. Consequently, the joint strength and hardness improved similarly. The joint strength also can be improved at higher traverse speed, because there were more plastic deformation and lower welding heat input.

It should be noted that increasing in traverse speed causes second phase precipitations to appear in the sample. They are located in the body of the grains. They have an elongated rounded shape ("Fig. 6").

According to conducted tensile tests, the fracture of welded joints occurs on the advancing side which may be related to more softening of this side of FSW joints. Furthermore, the higher values of hardness in retreating side can be seen in "Fig. 7". The weld zone and thermo-mechanically affected zone (TMAZ) are also shown in "Fig. 7".

3.4. Residual Stress Measurement

The residual stress measurements have been performed by hole-drilling strain gage method. The obtained results are listed in "Table 6".

Table 6 Residual values of different specimens

Specimen	Longitudinal residual stress (MPa)		
	Retreating Side	Weld Centerline	Advancing Side
R1120-T25	67.3	57.7	79.1
R1120-T31.5	69.6	60.71	95.5
R1600-T25	84.9	74.9	92.1
R1600-T31.5	85.2	76.7	110.2
	Transverse residual stress (MPa)		
	Retreating Side	Weld Centerline	Advancing Side
R1120-T25	-34.6	-55.2	-35
R1120-T31.5	-20	-34.1	8.3
R1600-T25	-64.3	-77.9	-53.1
R1600-T31.5	-32.3	-39.8	1.5

The tensile nature of longitudinal residual stress that aids to open the cracks tip can have a significant effect on the structure life [50]. Due to lower welding heat input in FSW process in compression to fusion welding processes [51-52], one of the main factors in creation of residual stress has been diminished. On the other hand, because of the pasty nature of the SZ and lower temperature gradient [53], further thermal stresses tend to relief.

As can be seen in Table 6, the mean longitudinal residual stress increases by increasing the rotation speed due to more generated heat and plastic deformation. The effect of rotation speed on longitudinal residual stress magnitude is larger three times than the effect of traverse speed. The strength of the welded joint enhanced by increasing the traverse speed. Despite of lower welding heat input, the longitudinal residual stress increased gradually. For instance, in constant rotation speeds of 1120 rpm and 1600 rpm, the longitudinal residual stress value increased about 5 and 2%, while increasing the traverse speed, respectively. Also, at constant traverse speeds of 31.5 mm/min and 25 mm/min, the longitudinal residual stress value increased about 30% and 26%, by increasing the rotational speed, respectively. The transverse residual stress did not show a clear dependence on tool speeds but the magnitudes are lower than longitudinal residual stress and weld zone is under compression in this direction. The transverse residual stress became more compressive by increasing the tool rotational speed and diminishing the tool transverse speed.

Furthermore, at advancing side, due to more generated heat and higher material flow [54], the residual stress of this side is higher than retreating side. It is another reason for occurrence of rupture at advancing side of AA2024 FSW joint. The magnitude of residual stress is in accordance with tensile test results. By increasing the traverse speed (causes increase in strain rate) and rotation speed (causes heating), residual stress increases subsequently.

4 CONCLUSIONS

Several joints were prepared by FSW of AA2024-T6 material. Results showed that the microstructures, hardness, tensile properties and residual stress are under influence of welding speed and related to each other. The following results were obtained:

1- An increment of rotation speed increases the grain size and results in finer and more homogenous distributions of particles in the weld SZ.
2- In minimum rotation speed and maximum traverse speed, the hardness of welding zone increases. This can be attributed to finer and homogenous distribution of second phase particles and precipitates and more plastic deformation of the weld zone.
3- The trend of tensile strength is similar to hardness; the maximum hardness and tensile strength were achieved at 31.5 mm/min transvers speeds and 1120 rpm rotation speed.
4- The defect free joints were ruptured in HAZ of advancing side. Higher residual stress in this side may be responsible for its lower strength.
5- In FSW of AA2024 T6, the grain size is important as induced plastic deformation and the second phase particles distribution which were the main factors that affected the mechanical properties.
6- By increasing of residual stresses, the tensile strength has decreased

ACKNOWLEDGMENTS

This study was financially supported by The Welding and Non-destructive testing applied research center (TWN), University of Tehran. The preparation of specimens, metallography analysis, residual stress measurement and mechanical tests were conducted in the TWN.

REFERENCES

[1] El-Sayed, M. M., Shash, A., Abd-Rabou, M., and ElSherbiny, M. G., Welding and Processing of Metallic Materials by Using Friction Stir Technique: A Review, Journal of Advanced Joining Processes, Vol. 3, 2021, pp. 100059, DOI: 10.1016/j.jajp.2021.100059.

[2] Kawashima, T., Sano, T., Hirose, A., Tsutsumi, S., Masaki, K., Arakawa, K., and et al., Femtosecond Laser Peening of Friction Stir Welded 7075-T73 Aluminum Alloys, Journal of Materials Processing Technology, Vol. 262, 2018, pp. 111-122, DOI: 10.1016/j.jmatprotec.2018.06.022.

[3] Lee, W. B., Yeon, Y. M., and Jung, S. B., The Improvement of Mechanical Properties of Friction-Stir-Welded A356 Al Alloy, Materials Science and Engineering: A, Vol. 355, 2003, pp. 154-159, DOI: 10.1016/S0921-5093(03)00053-4.

[4] Zhang, L., Zhong, H., Li, S., Zhao, H., Chen, J., and Qi, L., Microstructure, Mechanical Properties and Fatigue Crack Growth Behavior of Friction Stir Welded Joint of 6061-T6 Aluminum Alloy, International Journal of Fatigue, Vol. 135, 2020, pp. 105556, DOI: 10.1016/j.ijfatigue.2020.105556.

[5] Peng, P., Wang, W., Jin, Y., Liu, Q., Zhang, T., Qiao, K., and et al., Experimental Investigation on Fatigue Crack Initiation and Propagation Mechanism of Friction Stir Lap Welded Dissimilar Joints of Magnesium and Aluminum Alloys, Materials Characterization, Vol. 177, 2021, pp. 111176, DOI: 10.1016/j.matchar.2021.111176.

[6] Li, P., Chen, S., Dong, H., Ji, H., Li, Y., Guo, X., and et al., Interfacial Microstructure and Mechanical Properties of Dissimilar Aluminum/Steel Joint Fabricated Via Refilled Friction Stir Spot Welding, Journal of Manufacturing Processes, Vol. 49, 2020, pp. 385-396, DOI: 10.1016/j.jmapro.2019.09.047.

[7] Anthony, P., Reynolds, W. D., and Lockwood, T. U., SeidelProcessing-Property Correlation in Friction Stir Welds, Materials Science Forum, Vol. 331-337, 2000, pp. 1719-1724, DOI: 10.4028/www.scientific.net/MSF.331-337.1719.

[8] Shahmirzaloo, A., Farahani, M., and Farhang, M., Evaluation of Local Constitutive Properties of Al2024 Friction Stir-Welded Joints Using Digital Image Correlation Method, The Journal of Strain Analysis for Engineering Design, 2020, pp. 0309324720981201, DOI: 10.1177/0309324720981201.

[9] Pabandi, H. K., Jashnani, H. R., and Paidar, M., Effect of Precipitation Hardening Heat Treatment on Mechanical and Microstructure Features of Dissimilar Friction Stir Welded AA2024-T6 and AA6061-T6 Alloys, Journal of Manufacturing Processes, Vol. 31, 2018 pp. 214-220, DOI: 10.1016/j.jmapro.2017.11.019.

[10] Mehta, K. P., Patel, R., Vyas, H., Memon, S., and Vilaça, P., Repairing of Exit-Hole in Dissimilar Al-Mg Friction Stir Welding: Process and Microstructural Pattern. Manufacturing Letters, Vol. 23, 2020, pp. 67-70, DOI: 10.1016/j.mfglet.2020.01.002.

[11] Çelik, S., Tolun, F. Effect of Double-Sided Friction Stir Welding on The Mechanical and Microstructural Characteristics of AA5754 Aluminium Alloy, Materials Testing, Vol. 63, No. 9, 2021, pp. 829-835, DOI: 10.1515/mt-2021-0009.

[12] Hai, O. J., Conchita, K., Shigeo, S., Threadgill, P. L. Microstructure of Friction Stir Welded Joints in AA5182, Materials Science Forum, Vol. 331-337, 2000, pp. 1725-1730, DOI: 10.4028/www.scientific.net/MSF.331-337.1725.

[13] Yang, T., Wang, K., Wang, W., Peng, P., Huang, L., Qiao, K., and et al., Effect of Friction Stir Processing on Microstructure and Mechanical Properties of AlSi10Mg Aluminum Alloy Produced by Selective Laser Melting, JOM, Vol. 71, 2019, pp. 1737-1747, DOI: 10.1007/s11837-019-03343-9.

[14] Khodabakhshi, F., Arab, S., Švec, P., and Gerlich, A., Fabrication of a New Al-Mg/graphene Nanocomposite by Multi-Pass Friction-Stir Processing: Dispersion, Microstructure, Stability, And Strengthening, Materials Characterization, Vol. 132, 2017, pp. 92-107, DOI: 10.1016/j.matchar.2017.08.009.

[15] Narasimharaju, S., Sankunny, S., Microstructure and Fracture Behavior of Friction Stir Lap Welding of Dissimilar AA 6060-T5/Pure Copper, Engineering Solid Mechanics, Vol. 7, 2019, pp. 217-228, DOI: 10.5267/j.esm.2019.5.002.

[16] Kundu, J., Singh, H., Friction Stir Welding of Dissimilar Al Alloys: Effect of Process Parameters on Mechanical Properties, Engineering Solid Mechanics, Vol. 4, 2016, pp. 125-132, DOI: 10.5267/j.esm.2016.2.001.

[17] Shahani, A. R., Farrahi, A., Experimental Investigation and Numerical Modeling of The Fatigue Crack Growth in Friction Stir Spot Welding of Lap-Shear Specimen, International Journal of Fatigue, Vol. 125, 2019, pp. 520-529, DOI: 10.1016/j.ijfatigue.2019.04.026

[18] Peel, M., Steuwer, A., Preuss, M., and Withers, P. J., Microstructure, Mechanical Properties and Residual Stresses as A Function of Welding Speed in Aluminium AA5083 Friction Stir Welds, Acta Materialia, Vol. 51, 2003, pp. 4791-4801, DOI: 10.1016/S1359-6454(03)00319-7.

[19] Zhang, J., Upadhyay, P., Hovanski, Y., and Field, D. P., High-Speed Friction Stir Welding of AA7075-T6 Sheet: Microstructure, Mechanical Properties, Micro-Texture, and Thermal History, Metallurgical and Materials Transactions A, Vol. 49, 2018, pp. 210-222, DOI: 10.1007/s11661-017-4411-4.

[20] Sutton, M. A., Yang, B., Reynolds, A. P., and Taylor, R., Microstructural Studies of Friction Stir Welds in 2024-T3 Aluminum, Materials Science and Engineering: A, Vol. 323, 2002, pp. 160-166, DOI: 10.1016/S0921-5093(01)01358-2.

[21] Zhang, C., Cao, Y., Huang, G., Zeng, Q., Zhu, Y., Huang, X., and et al., Influence of Tool Rotational Speed on Local Microstructure, Mechanical and Corrosion Behavior of Dissimilar AA2024/7075 Joints Fabricated by Friction Stir Welding, Journal of Manufacturing Processes, Vol. 49, 2020, pp. 214-226, DOI: 10.1016/j.jmapro.2019.11.031.

[22] Bussu, G., Irving, P. E., The Role of Residual Stress and Heat Affected Zone Properties on Fatigue Crack Propagation in Friction Stir Welded 2024-T351 Aluminium Joints, International Journal of Fatigue, Vol. 25, 2003, pp. 77-88, DOI: 10.1016/S0142-1123(02)00038-5.

[23] Sowards, J. W., Gnäupel-Herold, T., McColskey, J. D., Pereira, V. F., and Ramirez, A. J., Characterization of Mechanical Properties, Fatigue-Crack Propagation, And Residual Stresses in A Microalloyed Pipeline-Steel Friction-Stir Weld, Materials & Design, Vol. 88, 2015, pp. 632-642, DOI: 10.1016/j.matdes.2015.09.049.

[24] Ilangovan, M., Rajendra Boopathy, S., and Balasubramanian, V., Effect of Tool Pin Profile on Microstructure and Tensile Properties of Friction Stir Welded Dissimilar AA 6061–AA 5086 Aluminium Alloy Joints, Defence Technology, Vol. 11, 2015, pp. 174-184, DOI: 10.1016/j.dt.2015.01.004.

[25] Farhang, M., Sam-Daliri, O., Farahani, M., and Vatani, A., Effect of Friction Stir Welding Parameters on The Residual Stress Distribution of Al-2024-T6 Alloy, Journal of Mechanical Engineering and Sciences, Vol. 15, No. 1, 2021, pp. 7684-7694, DOI: 10.15282/jmes.15.1.2021.06.0606.

[26] Bachmann, M., Carstensen, J., Bergmann, L., Dos Santos, J. F., Wu, C. S., and Rethmeier, M., Numerical Simulation of Thermally Induced Residual Stresses in Friction Stir Welding of Aluminium Alloy 2024-T3 at Different Welding Speeds, The International Journal of Advanced Manufacturing Technology, Vol. 91, No. 1, 2017, pp. 1443-1452. DOI: 10.1007/s00170-016-9793-8.

[27] Nazari, M., Besharati Givi, M. K., Farahani, M. R., Mollaei Milani, J., and Mohammad Zadeh, H., Investigation on the Effects of Using Nano-Size Al2O3 Powder on The Mechanical and Microstructural in The Multi-Passes Continuous Friction Stir Welding of the 2024-T6, Modares Mechanical Engineering, Vol. 14, No. 12, 2015, pp. 85-90, DOI: 20.1001.1.10275940.1393.14.12.1.2.

[28] Sam Daliri, O., Farahani, M., Characterization of Stress Concentration in Thin Cylindrical Shells with Rectangular Cut-out Under Axial Pressure, International Journal of Advanced Design and Manufacturing Technology, Vol. 2, 2017, pp. 133-141.

[29] Sam-Daliri, O., Farahani, M., and Farhang, M., A Combined Numerical and Statistical Analysis for Prediction of Critical Buckling Load of The Cylindrical Shell with Rectangular Cutout, Engineering Solid Mechanics, Vol. 7, No. 1, 2019, pp. 35-46.

[30] Elangovan, K., Balasubramanian, V., and Valliappan, M., Effect of Tool Pin Profile and Tool Rotational Speed on Mechanical Properties of Friction Stir Welded AA6061 Aluminium Alloy, Materials and Manufacturing Processes, Vol. 23, No. 3, 2008, pp. 251-260, DOI: 10.1080/10426910701860723.

[31] Krishna, M., Udaiyakumar, K., Kumar, D. M., and Ali, H. M., Analysis on Effect of Using Different Tool Pin Profile and Mechanical Properties by Friction Stir Welding on Dissimilar Aluminium Alloys Al6061 and Al7075, in IOP Conference Series: Materials Science and Engineering, 2018, pp. 012099, DOI: 10.1088/1757-899X/402/1/012099.

[32] Trimble, D., O'Donnell, G. E., and Monaghan, J., Characterisation of Tool Shape and Rotational Speed for Increased Speed During Friction Stir Welding of AA2024-T3, Journal of Manufacturing Processes, Vol. 17, 2015, pp. 141-150, DOI: 10.1016/j.jmapro.2014.08.007.

[33] Abd El-Hafez, H., Mechanical Properties and Welding Power of Friction Stirred AA2024-T35 Joints, Journal of Materials Engineering and Performance, Vol. 20, 2011, pp. 839-845, DOI: 10.1007/s11665-010-9709-y.

[34] Li, H., Yang, S., Zhang, S., Zhang, B., Jiang, Z., Feng, H., and et al., Microstructure Evolution and Mechanical Properties of Friction Stir Welding Super-Austenitic

Stainless Steel S32654, Materials & Design, Vol. 118, 2017, pp. 207-217, DOI: 10.1016/j.matdes.2017.01.034.

[35] Akbari, D., Farahani, M., and Soltani, N., Effects of the Weld Groove Shape and Geometry on Residual Stresses in Dissimilar Butt-Welded Pipes, The Journal of Strain Analysis for Engineering Design, Vol. 47, 2012, pp. 73-82, DOI: 10.1177/0309324711434681

[36] Sattari-Far, I., Farahani, M. R., Effect of the Weld Groove Shape and Pass Number on Residual Stresses in Butt-Welded Pipes, International Journal of Pressure Vessels and Piping, Vol. 86, No. 11, 2009, pp. 723-731, DOI: 10.1016/j.ijpvp.2009.07.007.

[37] Sabokrouh, M., Farahani, M., Experimental Study of The Residual Stresses in Girth Weld of Natural Gas Transmission Pipeline, Journal of Applied and Computational Mechanics, Vol. 5, No. 2, 2019, pp.199-206, DOI: 10.22055/JACM.2018.25756.1294.

[38] Sam-Daliri, O., Faller, L. M., Farahani, M., Roshanghias, A., Araee, A., Baniassadi, and et al., Impedance Analysis for Condition Monitoring of Single Lap CNT-Epoxy Adhesive Joint, International Journal of Adhesion and Adhesives, Vol. 88, 2019, pp. 59-65, DOI: 10.1016/j.ijadhadh.2018.11.003.

[39] Sam-Daliri, O., Farahani, M., Faller, L. M., and Zangl, H., Structural Health Monitoring of Defective Single Lap Adhesive Joints Using Graphene Nanoplatelets, Journal of Manufacturing Processes, Vol. 55, 2020, pp. 119-130, DOI: 10.1016/j.jmapro.2020.03.063.

[40] Stetco, C., Sam-Daliri, O., Faller, L. M., and Zangl, H., Piezocapacitive Sensing for Structural Health Monitoring in Adhesive Joints, 2019 IEEE International Instrumentation and Measurement Technology Conference (I2MTC), Auckland, New Zealand, 2019, pp. 1-5, DOI: 10.1109/I2MTC.2019.8827065.

[41] Sam-Daliri, O., Farahani, M., and Araei, A., Condition Monitoring of Crack Extension in The Reinforced Adhesive Joint by Carbon Nanotubes, Welding Technology Review, Vol. 91, No. 12, 2019, pp. 7-15, DOI: 10.26628/wtr.v91i12.1084.

[42] Rhodes, C. G., Mahoney, M. W., Bingel, W. H., Spurling, R. A., and Bampton, C. C., Effects of Friction Stir Welding on Microstructure of 7075 Aluminum, Scripta Materialia, Vol. 36, 1997, pp. 69-75, DOI: 10.1016/S1359-6462(96)00344-2.

[43] Murr, L. E., Liu, G., and McClure, J. C., A TEM Study of Precipitation and Related Microstructures in Friction-Stir-Welded 6061 Aluminium, Journal of Materials Science, Vol. 33, 1998, pp. 1243-1251, DOI:10.1023/A:1004385928163.

[44] Hadavi, M. R., Touski, H. Y., Jafari, H., and Ghasemi, F. A., Effect of Friction Stir Processing on Microstructure, Mechanical Properties, and Corrosion Fatigue Behavior of AA5083-H111 Metal Inert Gas Welded Joint, Journal of Materials Engineering and Performance, 2021, pp. 1-10, DOI: 10.1007/s11665-021-05783-4.

[45] Huang, K., Logé, R., A Review of Dynamic Recrystallization Phenomena in Metallic Materials, Materials & Design, Vol. 111, 2016, pp. 548-574, DOI: 10.1016/j.matdes.2016.09.012.

[46] El Rayes, M. M., Soliman, M. S., Abbas, A. T., Pimenov, D. Y., Erdakov, I. N., and Abdel-Mawla, M. M., Effect of Feed Rate in Fsw on The Mechanical and Microstructural Properties of AA5754 Joints, Advances in Materials Science and Engineering, Vol. 2019, 2019, pp. 1-12, DOI: DOI: 10.1155/2019/4156176.

[47] El-Danaf, E. A., El-Rayes, M. M., and Soliman, M. S., Friction Stir Processing: An Effective Technique to Refine Grain Structure and Enhance Ductility, Materials & Design, Vol. 31, 2010, pp. 1231-1236, DOI: 10.1016/j.matdes.2009.09.025.

[48] Lu, Y., Wang, J., Li, X., Chen, Y., Zhou, D., Zhou, G., et al., Effect of Pre-Deformation on The Microstructures and Properties of 2219 Aluminum Alloy During Aging Treatment, Journal of Alloys and Compounds, Vol. 699, 2017, pp. 1140-1145, 10.1016/S1003-6326(12)61733-6, DOI: 10.1016/j.jallcom.2016.12.006.

[49] Borrego, L., Costa, J., Jesus, J., Loureiro, A., and Ferreira, J., Fatigue Life Improvement by Friction Stir Processing of 5083 Aluminium Alloy MIG Butt Welds, Theoretical and Applied Fracture Mechanics, Vol. 70, 2014, pp. 68-74, DOI: 10.1016/j.tafmec.2014.02.002.

[50] Zamanpour, A., Farahani, M., Farhang, M., and Vafa, N., Experimental Study on the Effects of Harmonic Vibration on the Stress Relief of the Butt Welded AISI 1021 Pipes. Iranian Journal of Manufacturing Engineering, Vol. 7, No. 2, 2020, pp. 1-7, http://www.iranjme.ir/article_108087.html.

[51] Enami, M., Farahani. M., and Farhang, M., Novel Study on Keyhole Less Friction Stir Spot Welding of Al 2024 Reinforced with Alumina Nanopowder, The International Journal of Advanced Manufacturing Technology, Vol. 101, No. 9, 2019, pp. 3093-3106, DOI: 10.1007/s00170-018-3142-z.

[52] Farhang, M., Farahani. M., and Enami, M., Experimental Study on the Effects of Friction Stir Spot Welding Process Parameters on AL2024T3 Joint Strength. ADMT Journal, Vol. 14, No. 4, 2021, pp. 105-112,DOI:10.30495/ADMT.2021.1922979.1280.

[53] Farhang, M., Farahani. M., and Nazari M., Incorporation of Al2O3 Powder for Improvement of The Mechanical and Metallurgical Properties of Multi-Passes Friction Stir Welding of Al 2024. Iranian Journal of Manufacturing Engineering, Vol. 8, No. 3, 2021, pp.35-46, http://www.iranjme.ir/article_133594.html?lang=en.

[54] Zhai, M., Wu, C., and Su, H., Influence of Tool Tilt Angle on Heat Transfer and Material Flow in Friction Stir Welding, Journal of Manufacturing Processes, Vol. 59, 2020, pp. 98-112, DOI: 10.1016/j.jmapro.2020.09.038.